Materials Science in Semiconductor Processing 46 (2016) 6–9

Contents lists available at ScienceDirect

Materials Science in Semiconductor Processing

journal homepage: www.elsevier.com/locate/mssp

Phase transition of Cu_2O to CuO nanocrystals by selective laser heating

Thi Ha Tran [a], Viet Tuyen Nguyen [b,c,*]

[a] Faculty of General Sciences, Hanoi University of Mining and Geology, Tu Liem, Hanoi, Vietnam
[b] Duy Tan University, 182 Nguyen Van Linh, Danang, Vietnam
[c] Physics Faculty, Vietnam National University – University of Science, 334 Nguyen Trai, Thanh Xuan, Hanoi, Vietnam

ARTICLE INFO

Article history:
Received 20 December 2015
Received in revised form
17 January 2016
Accepted 29 January 2016

Keywords:
Cupric oxide
Microwave irradiation method
Laser annealing
Raman spectra

ABSTRACT

In this paper, we reported the preparation of CuO nanocrystals by microwave irradiation method. With the aid of suitable surfactants, CuO nanoparticles of uniform size and shape were successfully prepared. The as-prepared nano-products were characterized by different techniques such as Xray diffraction (XRD), Raman scattering, scanning electron microscopy (SEM), which all confirmed the good quality of the product. However, Raman spectra showed some peaks, which were attributed to impurity phases such as Cu_2O or $Cu(OH)_2$. Post annealing the samples by laser is a good method to convert these phases into pure CuO. Phase transition was observed *in situ* by Raman spectroscopy. After laser treatment process, Raman spectra of the samples showed that the nano-product is single phase and the crystal quality of CuO nanocrystal was improved clearly.

1. Introduction

Cupric oxide (CuO) is a transition metal oxide semiconductor of monoclinic structure. CuO was well-known for applications in catalyst and thermal conducting fields but recently new potential applications of this material such as high temperature superconductivity, lithium ion batteries, sensors and solar cells [1–6] have renewed a great interest from scientists. Furthermore, many interesting properties of CuO, which are enhanced in nanomaterials, make it a hot topic in different science and engineer fields.

Although great progress has been achieved in preparing different nanostructures of cupric oxide, exploring different approaches to seek for a good method to prepare CuO nanostructures still requires much effort from material scientists. A quick, high throughput process to synthesize nanomaterials of high quality at a large scale not only makes it easier to study the properties of the materials but also paves the way to realize the commercial applications. In this paper, we report the fabrication of CuO nanoparticles by a quick process using microwave irradiation. The product has uniform size and shape as well as good quality, as shown by different characterization techniques: Xray diffraction, Scanning electron and Raman scattering microscopy. The quality of the product can be further improved by post annealing under laser illumination to remove undesired phases from the nanoproduct.

2. Experiment

The detail process to synthesize CuO nanostructures by microwave method could be found elsewhere [7]. Typically, 50 ml of copper acetate (Merk, 99% purity) 0.2 M was continuously magnetic stirred at constant rate. Meanwhile, 50 ml of 0.4 M NaOH in ethanol (Merk, 99% purity) was added dropwise. In case of using surfactants, suitable amount of polyethylence glycol (PEG) or polyvinyl pyrrolidone (PVP) was dissolved into copper salt solution before reaction with sodium hydroxide. The resulting solution was then heated by microwave irradiation in 10 min at microwave power of 80 W to obtain CuO nano product. A dark precipitation was collected at the end of the heating process. The washing process was repeated several times with distilled water and ethanol to obtain pure product. Finally the product was dried to obtain CuO nanopowder or drop-casted on sodalime glass to obtain thin films of nanocrystals for further characterization. Three CuO nanoparticle samples were prepared without surfactant (M1), with PEG (M2) and PVP (M3) as surfactants.

The particle morphologies and structures of the products were investigated by a scanning electron microscope (SEM 1010-JEOL) and X-ray diffractometer (Bruker-AXS D5005). Raman measurements at room temperature were carried out by using Horiba Jobin Yvon spectrometer with several excitation wavelengths: 632.8 nm-line of He-Ne; 514.5 nm-line of Ar ion and 441.6 nm-line of He-Cd laser.

* Corresponding author at: Physics Faculty, Vietnam National University – University of Science, 334 Nguyen Trai, Thanh Xuan, Hanoi, Vietnam

http://dx.doi.org/10.1016/j.mssp.2016.01.021
1369-8001/

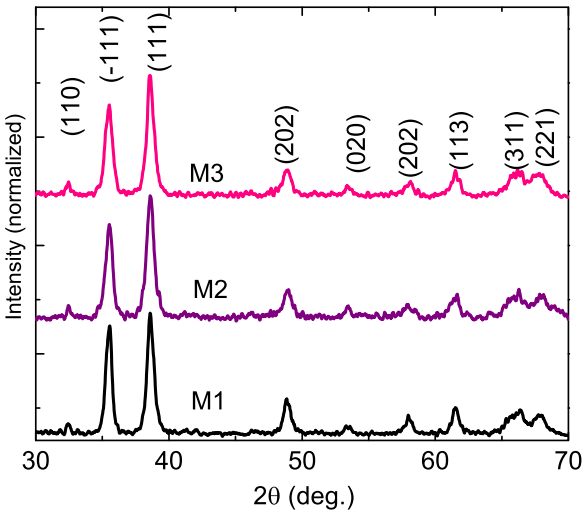

Fig. 1. Xray diffraction patterns of the as-prepared samples.

3. Results and discussion

Xray diffraction patterns of the three samples are shown in Fig. 1. To the limitation of XRD measurement, all of the samples show characteristic peaks of CuO without additional peaks of other phases. Clear peaks in the patterns imply that the crystallinity of the nanoproducts is good. Crystal size estimated by using Debye Sherre formula are 16, 12, 11 nm for the samples prepared without surfactant, with PEG and PVP, respectively.

The influence of surfactants on the morphology of nanoproducts could be observed directly through SEM images of the samples. As can be seen from Fig. 2, particle size is much smaller for the samples prepared with surfactants, especially for sample prepared with PVP. Furthermore, samples prepared with PEG and PVP also show better uniformity in size and shape. The fact that, size of products decreases from around one micron to around one hundred nanometer when using PVP as surfactant, demonstrates the important role of surfactant on the morphology of nanoproduct.

After the nucleation and growth process are completed, the average size of CuO nanoparticles could continue to increase due to agglomeration. As the nanoparticles were agglomerated it is difficult to separate them. In order to obtain product of high quality, it is necessary to stabilize the as-produced nanostructures. There are two main stabilization mechanisms: electrostatic and steric stabilization. While most polymers could only provide steric stabilization, some others show advantages of providing both stabilization mechanisms simultaneously. Many groups had taken advantages of such combination by using certain polymers of high ion density. The ionic nature of the polymer provides the electrostatic repulsion between nanoparticles while the long polymer chain keeps the nanoparticles away from each other by steric effect. Among the polymers of this kind, PVP is one of the most commonly used as it can be dissolved in both polar and non-polar solvents. The polar amide group in polymeric chain of PVP is readily attached to the surface of nanoparticles to protect them from aggregation by the two stabilization mechanism. The improvement in homogeneity and uniformity of nanoproduct prepared by PVP compared with PEG could be explained by the above understanding on the role of different type of polymer. PEG could mostly provide steric repulsion as it has less ionic nature, which also means that PEG could not produce as strong electrostatic repulsion as PVP.

The following measurements were conducted only on the sample of highest quality (M3). Along with Xray diffraction, Raman spectroscopy, which is a sensitive probe to the local atomic arrangements and vibrations of the materials, has been also widely used to investigate the microstructural nature of the nano-sized materials. Raman scattering also provides useful information about the structures and bonds of materials. In particular for CuO nanomaterial, Raman scattering could help to show the crystallinity of the product or detect the existence of undesired phases such as Cu_2O or $Cu(OH)_2$ at a much lower content compared with limit of detection of Xray diffraction measurement. The space group of CuO is C_{2h}^6 with two molecules per primitive cell so the zone center Raman active normal modes of CuO are $\Gamma_{RA}=4A_u+5Bu+A_g+2B_g$. Among these vibration modes, there are three acoustic modes (A_u+2B_u), six infrared active modes ($3A_u+3B_g$), and three Raman active modes (A_g+2B_g). Three well known Raman bands of CuO are A_g (296 cm^{-1}), B_{1g} (346 cm^{-1}), and B_{2g} (631 cm^{-1}) [8]. Fig. 3 shows Raman spectra of sample M3, taken with three different excitation wavelengths 623.8, 514.5, 441.6 nm. In these spectra, A_{1g} and B_{1g} modes of CuO agreed well with other reports for CuO bulk material. No peak shift due to phonon confinement effect was observed because particle size did not reach closed enough to the Bohr exciton radius of CuO, which is quite small, and in the range from 6.6 to 28.7 nm [9]. However, an additional peak appeared at around 590 cm^{-1} and convoluted with the B_{2g} peak of CuO to form a broad band.

From theoretical point of view, the occurrence of defects in a crystalline material can break the translational symmetry of the crystal lattice or totally lost material long range order in the extreme case where material is in glassy or amorphous state. Such these changes will lead to variation in Raman selection rules for perfect crystal and could give rise to the appearance/disappearance of some Raman modes. In fact, these changes are rarely observed experimentally because the density of defect is not enough to make a significant perturbation to the vibration properties of materials. However, oxide of copper is an exception as defect induced vibration modes was reported for this material

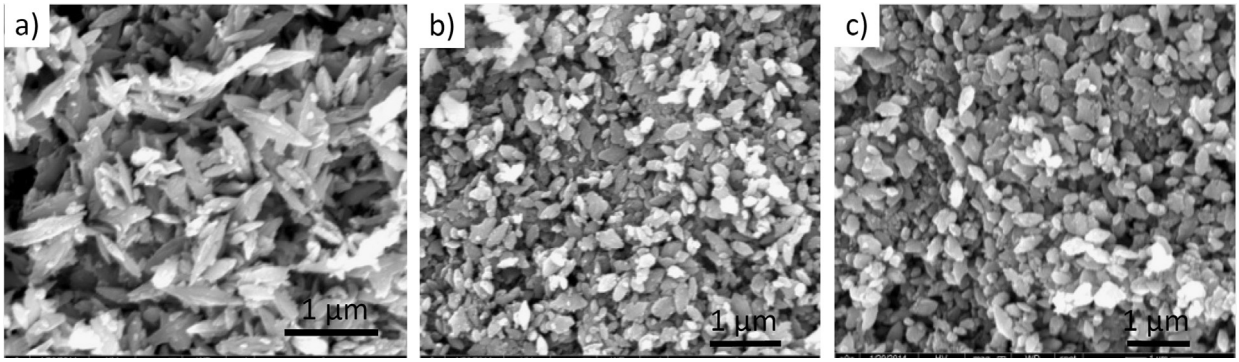

Fig. 2. SEM images of CuO nanostructure samples: (a) M1, (b) M2 and (c) M3.

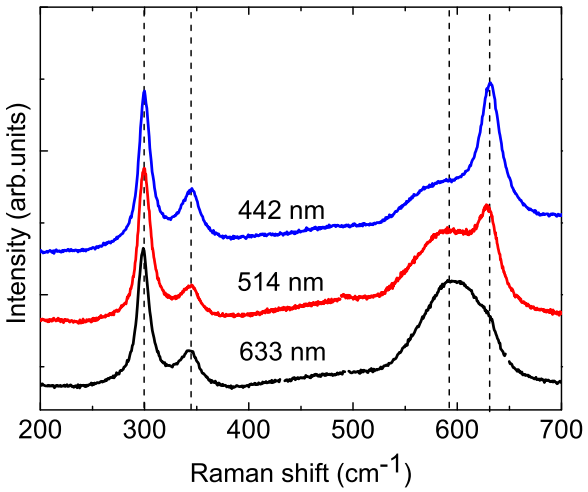

Fig. 3. Raman spectra of sample M3 taken with different excitation wavelengths: 633 nm, 514 nm, 442 nm.

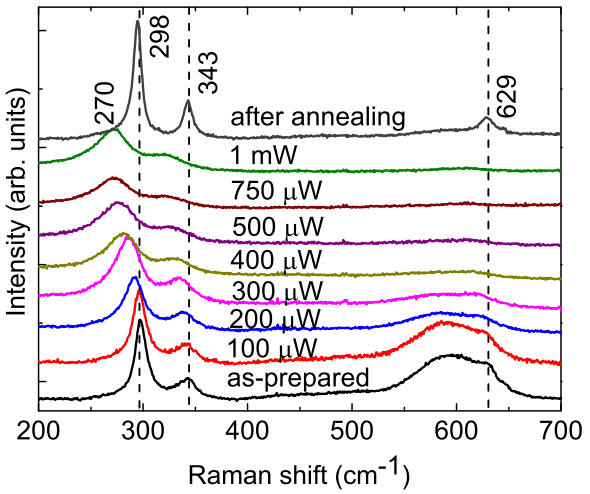

Fig. 4. In situ Raman observation of sample M3 under laser treatment at different laser power.

[10]. Hence, the broad Raman feature as observed in this case may come from defects on the surface of the nanostructures or from unintended phases such as Cu_2O [11] or $Cu(OH)_2$ [12].

The penetration depth of each laser on a semiconductor sample depends on the absorption coefficient corresponding to the wavelength and can be roughly given by $1/2\alpha$, where α is the absorption coefficient and factor 1/2 should be added to the formula as return path of light must be taken into account for backscattering configuration. As the excitation energy get closer to the bandgap energy of semiconductor, absorption coefficient gets higher and the penetration depth decrease rapidly and hence Raman signal will be collected mostly on the surface of samples.

When changing from red to green and blue laser, of which penetration depth decreases respectively, the intensity of the peak at lower side of 600 cm^{-1} broad band decreased gradually. Hence if the peak at 600 cm^{-1} belongs to defect, the intensity of this peak should increase as normally defects are distributed on the surface of nanoparticles. In fact, the intensity of this peak decreased as observed in the Raman spectra taken with different excitation wavelength, we therefore believe that this peak come from unintended phases rather than from defects of the nanoproduct. The reason for the enhancement of Raman intensity of this peak, which was assigned as Cu_2O maybe because 632.8 nm laser (1.95 eV) match better to the bandgap of Cu_2O (2.17 eV) [13] than other wavelengths used in this paper. Another explanation is the nanoproducts have core/shell structures of the form Cu_2O/CuO, that make the Raman signal of the inner core of Cu_2O could be detected when using red laser of higher penetration depth. Additional measurements are necessary to clarify the origin in the dependence of Raman intensity on excitation wavelengths.

Energy dispersive spectroscopy showed that the ratio of oxygen to copper atoms is slightly less than 1 or in other words, the samples are rich in copper and slightly oxygen deficient. This result is in agreement with our explanation for the formation of Cu_2O in the samples. Therefore, post annealing is necessary to convert Cu_2O phase into pure CuO. The post annealing was done by shining a laser beam of high density on the sample and the phase transition was observed – *in situ* by Raman spectra. The main advantage that laser annealing offers over the conventional heating is selective heating of the sample i.e. one can heat the sample without heating the substrate as laser beam is very spatially defined so that it helps to control well the desired heating area. Further more, by choosing the correct wavelength of the laser beam, heating process can be controlled through the depth of the samples base on the dependence of penetration depth on absorption coefficient as presented above. In general, short wavelength photons (near the band gap of semiconductor) will be absorbed mostly near the surface of material and could generate more heat in the shining area. These advantages help to minimize the waste energy for the annealing process and hence the annealing process can be done in several minutes as in our case in stead of hours in normal heating process.

Fig. 4 shows the Raman spectra of the CuO nanostructure (sample M3) under illumination of 633 nm laser of different laser density. As can be seen in the figure, the phase transition could be observed clearly when increasing the density of the shinning laser beam. Peaks of Cu_2O gradually disappear under higher illumination power. At the same time, the A_1 peak of CuO broadens and shifts to low wave number, which could be understood as the effect of heating. When being heated, the lattice expands and the force constant should decrease, the vibrating frequency will be red shifted.

One more thing to note here is that a quite low power of several hundreds of microwatts could results in peaks shifts due to heating effect, it is perhaps some of the reported applications of Raman studies of CuO nanostructures seemed to neglect the possible effect of heating, which becomes more significant under confocal measurement where laser beam is localized in a small region and heat dissipation is not enough due to the isolation of nanostructures.

The oxidation kinetics of Cu_2O could be described by several laws such as parabolic law [14], cubic law [15] or most recently by the logarithmic law suggested by Zhu et al. [16]. The logarithmic oxidation rate law results from grain-boundary diffusion in the oxide layers. According to Zhu et al., the activation energy for Cu_2O oxidation is relatively high in the lower-temperature range (600–800 °C), but becomes very small or even negative at higher temperatures (800–1050 °C), which is more favorable for the oxidation of Cu_2O into CuO. The very small or negative activation energies in the higher-temperature range can be attributed to the very small thermodynamic driving force and the fast lateral growth of CuO grains related to a sintering effect. Such high temperatures, which is required to activate the oxidation of Cu_2O, could be realized by illuminating the sample with a high density beam of laser. In this case, the energy of laser beam at power of 0.3 mW is enough to activate the reaction of transform Cu_2O into CuO and higher the power results in higher the oxidation rate.

At power density of 500 μW, Cu_2O or $Cu(OH)_2$ phase was totally removed from the sample as can be seen by comparing the Raman spectra of the sample before and after annealing which were

measured at the same condition. After annealing, the broad peak at 600 cm^{-1} were replaced by the peak B_{2g} of CuO and all Raman peak of CuO become more intense and sharper, which implies that the crystalinity of the samples was improved greatly after heat treatment.

4. Conclusion

In conclusion, we had successfully synthesized CuO nanoparticles via a simple process using microwave irradiation. By using PVP as surfactant, size of nanostructures could be reduced from around 1 μm when no surfactant is used, to 100 nm with narrow size distribution. Both Xray diffraction pattern and Raman spectroscopy confirmed the high crystal quality of the product. Phonon confinement effect was not observed in Raman spectra. Instead, there is a small amount of undesired phases such as Cu_2O, $Cu(OH)_2$ in the product, which may exist in form of Cu_2O/CuO core/shell structure as suggested by Raman spectra with different excitation wavelength. Rapid thermal treatment by laser seems to be a good way to convert the remaining unintended phases into CuO to give nanoproduct of pure phase and high crystalinity.

Acknowledgement

The authors would like to thanks Faculty of Physics, Vietnam National University – University of Science and Opto-electronic and Semiconductor Laboratory, Faculty of Physics, Sogang University, Korea for letting us using the equipment.

References

[1] X. Wang, X. Xu, Thermal conductivity of nanoparticle–fluid mixture, J. Thermophys. Heat Transf. 13 (1999) 474–480.
[2] A.K. Rai, L.T. Anh, J. Gim, V. Mathew, J. Kang, B.J. Paul, N.K. Singh, J. Song, J. Kim, Facile approach to synthesize CuO/reduced graphene oxide nanocomposite as anode materials for lithium-ion battery, J. Power Sources 244 (2013) 435–441.
[3] A. Aslanin, V. Oroojpour, CO gas sensing of CuO nanostructures synthesized by an assisted solvothermal wet chemical route, Physica B 406 (2011) 144–149.
[4] Y. Li, J. Liang, Z. Tao, J. Chen, CuO particles and plates: Synthesis and gas-sensor application, Mater. Res. Bull. 43 (2008) 2380–2385.
[5] V. Kumar, S. Masudy-Panah, C.C. Tan, T.K.S. Wong, D.Z. Chi, G.K. Dalapati, Copper oxide based low cost thin film solar cells, in: Proceedings of the Nanoelectronics Conference (INEC), IEEE 5th International, 2013.
[6] H. Kidowaki, T. Oku, T. Akiyama, A. Suzuki, B. Jeyadevan, J. Cuya, Fabrication and characterization of CuO-based solar cells, J. Mater. Sci. Res. 1 (2012) 138–143.
[7] T.T. Ha, T.D. Canh, N.V. Tuyen, A quick process for synthesis of ZnO nanoparticles with the aid of microwave irradiation, ISRN Nanotechnology 2013 (2013) 497873(1)–497873(7).
[8] M.A. Dar, Q. Ahsanulhaq, Y.S. Kim, J.M. Sohn, W.B. Kim, H.S. Shin, Versatile synthesis of rectangular shaped nanobat-like CuO nanostructures by hydrothermal method; structural properties and growth mechanism, Appl. Surf. Sci. 255 (2009) 6279–6284.
[9] S.P. Meshram, P.V. Adhyapak, U.P. Mulik, D.P. Amalnerkar, Facile synthesis of CuO nanomorphs and their morphology dependent sunlight driven photocatalytic properties, Chem. Eng. J. 204–206 (2012) 158–168.
[10] T. Sander, C.T. Reind, M. Giar, B. Eifert, M. Heinemann, C. Heiliger, P.J. Klar, Correlation of intrinsic point defects and the Raman modes of cuprous oxide, Phys. Rev. B 90 (2014) 045203(1)–045203(8).
[11] Z.H. Gan, G.Q. Yu, B.K. Tay, C.M. Tan, Z.W. Zhao, Y.Q. Fu, Preparation and characterization of copper oxide thin films deposited by filtered cathodic vacuum arc, J. Phys. D: Appl. Phys. 37 (2004) 81–85.
[12] Archana Chaudhary, Harish C. Barshilia, Nanometric multiscale rough CuO/Cu$(OH)_2$ superhydrophobic surfaces prepared by a facile one-step solution-immersion process: transition to superhydrophilicity with oxygen plasma treatment, J. Phys. Chem. C 115 (2011) 18213–18220.
[13] L. Liao, B. Yan, Y.F. Hao, G.Z. Xing, J.P. Liu, B.C. Zhao, Z.X. Shen, T. Wu, L. Wang, J. T.L. Thong, C.M. Li, W. Huang, T. Yu, P-type electrical, photoconductive, and anomalous ferromagnetic properties of Cu_2O nanowires, Appl. Phys. Lett. 94 (2009) 13106 [1)-13106(3].
[14] J.L Meijering, M.L Verheijke, Oxidation kinetics in the case of ageing oxide films, Acta Metall. 7 (1959) 331–338, http://dx.doi.org/10.1016/0001-6160(59)90199-3.
[15] K. Hauffe, P. Kofstad, Über den mechanismus der oxydation von Cu_2O bei hohen temperaturen, Zeischrift Elektrochem. 59 (1955) 399–404.
[16] Y. Zhu, K. Mimura, M. Isshiki, Oxidation mechanism of Cu_2O to CuO at 600–1050 °C, Oxid. Met. 62 (2004) 207–222.